Vavilov-Cherenkov effect in a driven resonant medium

M. Artoni,[1,2] I. Carusotto,[3,4] G. C. La Rocca,[4] and F. Bassani[4]
[1]*INFM–European Laboratory for Non-linear Spectroscopy, Sesto Fiorentino, 50019 Firenze, Italy*
[2]*INFM–Department of Chemistry and Physics of Materials, Via Valotti 9, 25133, Brescia, Italy*
[3]*Laboratoire Kastler Brossel, École Normale Supérieure, 24 rue Lhomond, 75231 Paris Cedex 05, France*
[4]*INFM–Scuola Normale Superiore, Piazza dei Cavalieri 7, 56126 Pisa, Italy*
(Received 9 August 2002; published 21 April 2003)

The Vavilov-Cherenkov effect in a dispersive and resonant absorbing medium is substantially modified by the presence of an external electromagnetic field. Depending on the field parameters and configuration we anticipate a remarkable increase of the emission yield at resonance. Our predictions are implemented by numerical estimates for cuprous oxide (Cu_2O) where the yield turns out to be one to two orders of magnitude that obtained in the absence of the field.

DOI: 10.1103/PhysRevE.67.046609 PACS number(s): 42.25.Bs, 41.60.Bq

I. INTRODUCTION

In a transparent uniform medium a charged particle moving with a constant speed v above a critical velocity emits an unusual type of coherent radiation that was first observed by Vavilov [1] and Cherenkov [2] in liquid media. The phenomenon was later interpreted by Frank and Tamm [3]. They showed that a charge traveling faster than the speed of light in a medium with frequency-independent refractive index emits radiation displaying a shockwave singularity at the surface of a circular cone. The angle subtended by the cone is directly determined by the ratio between the speed of light in the medium and that of the particle through the familiar Cherenkov coherence condition [4,5]. This cone is essentially analogous to the Mach cone that characterizes a shockwave produced by the motion of a supersonic source in air or other media [6].

The study of such an effect was further extended to other materials where the emission of Cherenkov radiation turns out to be a very small fraction of the total energy lost by the moving charge [7]. The loss of the particle energy in transparent solids, e.g., mainly arises in fact from the ionization or excitation of the polarizable medium [8–10], yet the small fraction of energy loss due to the emission of Cherenkov radiation can still be singled out [7,11] from the particle's total losses owing to its directionality.

The situation becomes furthermore involved in dispersive media. Expressions for the emission yield and threshold conditions in a dispersive and transparent medium were first derived by Tamm [12] and partly by Fermi [13]. Budini [7] further showed that in a dispersive and absorbing medium described by a complex dielectric function $\epsilon(\omega)$ it is necessary to take into account the damping of the bound electrons of the polarizable medium in order to account for the energy lost by Cherenkov emission besides that lost by excitation and ionization of the polarizable medium. Following rather general arguments he introduced the threshold condition $v^2 > c^2/\mathrm{Re}[\epsilon(\omega)]$ and an expression for the radiated energy which reduces to the Frank and Tamm results [3,12] in the case of a perfectly transparent medium. Over the years the effect of Cherenkov emission in dispersive media has drawn very little attention apart from some work aiming to clarify the role of phase and group velocity in the emission process [14] as well as intriguing emission features in media with negative group velocities [15], or apart from some more recent work predicting drastic narrowing of the Cherenkov group cone [16] in a coherently driven ultracold atomic gas [17] as well as the possibility of emission at speeds below threshold [18]. Cherenkov emission at subluminal speeds, in particular, has recently been observed experimentally [19] by using optically generated moving dipoles in nonlinear crystals at very low temperatures.

The present work focusses on the influence of an *external* electromagnetic field on the Cherenkov effect for a certain class of dispersive and resonant absorbing solid media. The presence of the field alters the form of the dielectric function by modifying the medium's absorptive and dispersive properties and by reducing its symmetry, which makes the actual dielectric function, in general, anisotropic. We here anticipate that both modifications may lead to a significant change of the resonant emission yield as well as to a change of the emission coherence and threshold conditions that the medium would otherwise exhibit in the absence of the field. Modifications of the medium dispersion, in particular, give rise to propagation at rather slow group velocities that also affect the Cherenkov emission pattern; this effect, which has already been predicted to occur for a charged particle moving across an ultracold cloud of alkali atomic gas [17], will not be addressed here.

The purpose of this paper is thus twofold. *First*, we adopt a classical electrodynamics approach based on the dielectric function to develop a general theory for Cherenkov energy losses in the presence an external laser field in dispersive and resonant absorbing materials. *Second*, we provide numerical results for Cu_2O where the presence of the field allows for a substantial increase of the emission yield in the resonance region where the observation of Cherenkov radiation would otherwise be more difficult. We examine, in particular, the dependence of the emission enhancement on the external field configuration and on the particle incident direction.

We derive in Sec. II the field radiated by the charged particle via a straightforward solution of Maxwell equations. The particle energy loss function and the relevant coherence and threshold conditions are derived and discussed in Sec.

III. We give in Sec. IV the dielectric functions for Cu_2O appropriate to two different external field configurations of experimental interest while the relevant numerical results are presented and discussed in Sec. V. Detailed calculations needed to derive the general results of Secs. II and III are reported in three appendixes.

II. THE RADIATED FIELDS

The external electric field modifies the dielectric function so as to make it anisotropic in place of the isotropic one that the medium would have in the absence of the external field. The specific configurations that we will examine in the following sections are amenable to experiments with Cu_2O and amount to considering a *uniaxial* [20] dielectric function. We will then restrict our analysis to the case of a dispersive and resonant absorbing uniaxial medium where *x*, *y*, and *z* denote the medium principal axes. We take the external electric field linearly polarized along $\hat{x}$ which determines the direction of the optical *c* axis (See Fig. 1). We assume in the following that the particle velocity has a positive component along $\hat{x}$ and a non-negative component along $\hat{y}$. This, along with the particular case of a velocity orthogonal to the optical *c* axis treated separately in Appendix B, is expected to exhaust most common experimental situations [4]. Taking advantage of the medium's cylindrical symmetry about the $\hat{x}$ axis we find it convenient to express the electric field $\mathbf{E}(\mathbf{r},t)$ as

$$\mathbf{E}(\mathbf{r},t)=\frac{1}{(2\pi)^3}\int d\boldsymbol{k}_\perp \int d\omega\, e^{i\boldsymbol{k}_\perp\cdot\mathbf{r}-i\omega t}\boldsymbol{E}_{\boldsymbol{k}_\perp,\omega}(x), \quad (1)$$

where $\boldsymbol{k}_\perp=(k_y\hat{y}+k_z\hat{z})$ denotes the projection of the emitted radiation wave vector $\boldsymbol{k}$ in the principal plane. Analogous expansions hold for the fields $\mathbf{D}(\mathbf{r},t)$, $\mathbf{B}(\mathbf{r},t)$, and $\mathbf{H}(\mathbf{r},t)$ as well as for the free charge density

$$\rho(\mathbf{r},t)=q_e\delta(z)\,\delta(x-v_xt)\,\delta(y-v_yt), \quad (2)$$

and for the free current density

$$\mathbf{J}(\mathbf{r},t)=q_e\boldsymbol{v}\,\delta(z)\,\delta(x-v_xt)\,\delta(y-v_yt). \quad (3)$$

The particle is here assumed to be a point charge q_e moving with velocity $\boldsymbol{v}$ along a direction that is perpendicular to the *z* axis as shown in Fig. 1.

The energy lost by the charge through the medium is typically much smaller than its kinetic energy and we may then neglect the small decrease of the charge velocity (*Born approximation*). The Maxwell equations for these charge and current densities and a uniaxial dielectric tensor characterized by longitudinal and transverse components $\epsilon_\parallel(\omega)$ and $\epsilon_\perp(\omega)$ can be solved and after some lengthly algebra, which we report in Appendix A, they acquire the form

$$\left(-\frac{\epsilon_\parallel}{\epsilon_\perp}\partial_x^2-\epsilon_\parallel\frac{\omega^2}{c^2}+\boldsymbol{k}_\perp^2\right)E_x(x)=\frac{4\pi iq_e}{c^2}\left(\frac{-k_xc^2}{v_x\epsilon_\perp}+\omega\right)e^{ik_xx}, \quad (4)$$

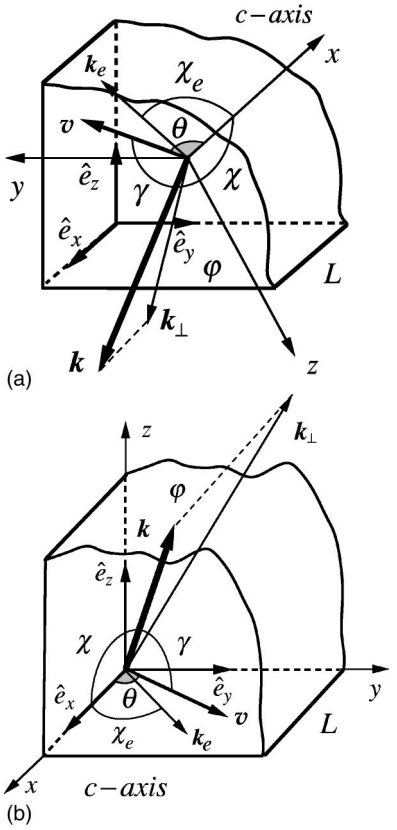

FIG. 1. A fast charged particle traverses a layer of thickness *L* of a medium coherently driven by an external laser field which makes the medium *uniaxial*. The principal axes $\hat{x}$, $\hat{y}$, and $\hat{z}$ are oriented in the direction [1,1,1], [1,−1,0], and [1,1,−2] (upper frame) and [1,0,0], [0,1,0], and [0,0,1] (lower frame) with respect to the crystal cubic axes $\hat{e}_x$, $\hat{e}_y$, and $\hat{e}_z$. The external field propagates in the *y*-*z* plane (principal plane) and is linearly polarized along *x* (optical *c* axis). The particle velocity $\boldsymbol{v}$ lies in the *x*-*y* plane making an angle θ (shaded sector) about the optical *c* axis. Cherenkov emission occurs in the direction of the wave vector $\boldsymbol{k}$ at an angle χ about the optical *c* axis while $\boldsymbol{k}_\perp$ denotes the wave vector projection on the principal plane.

$$\left(-\partial_x^2-\epsilon_\perp\frac{\omega^2}{c^2}+\boldsymbol{k}_\perp^2\right)E_y(x)=ik_y\epsilon_r\partial_xE_x-\frac{4\pi iq_e}{c^2}\times\left(\frac{k_yc^2}{v_x\epsilon_\perp}-\frac{\omega v_y}{v_x}\right)e^{ik_xx}, \quad (5)$$

$$\left(-\partial_x^2-\epsilon_\perp\frac{\omega^2}{c^2}+\boldsymbol{k}_\perp^2\right)E_z(x)=ik_z\epsilon_r\partial_xE_x-\frac{4\pi iq_e}{c^2}\left(\frac{k_zc^2}{v_x\epsilon_\perp}\right)e^{ik_xx}, \quad (6)$$

where we introduce the reduced dielectric tensor

$$\epsilon_r=\frac{\epsilon_\parallel}{\epsilon_\perp}-1. \quad (7)$$

We also recall here the component of the wave vector $\boldsymbol{k}$ along the optical c axis as given in Eq. (A7),

$$k_x = \frac{\omega - k_y v_y}{v_x}, \tag{8}$$

and relating [21] the frequency and direction of the emitted radiation to the charged particle speed. The frequency dependencies of all dielectric functions are not shown here, while

$$E_{\{x,y,z\}}(x) = E_{\boldsymbol{k}_\perp,\omega}(x)\big|_{\{x,y,z\}} \tag{9}$$

is a shorthand notation for the electric field components. Equations (4) and (5) can now be solved and the corresponding single Fourier components of the electric field can be written as

$$E_x(x) = \frac{q_e}{c^2}\left(\omega - \frac{k_x c^2}{v_x \epsilon_\perp}\right)\frac{4\pi i}{q_\parallel^2} e^{ixk_x} \tag{10}$$

and

$$E_y(x) = \frac{q_e}{c^2}\left[\omega\frac{v_y}{v_x} - \frac{k_y c^2}{v_x \epsilon_\perp} - \left(1 - \frac{\epsilon_\parallel}{\epsilon_\perp}\right) \times \left(-\omega + \frac{k_x c^2}{v_x \epsilon_\perp}\right)\frac{k_x k_y}{q_\parallel^2}\right]\frac{4\pi i}{q_\perp^2} e^{ixk_x}, \tag{11}$$

with

$$q_\parallel^2 = \boldsymbol{k}_\perp^2 - \epsilon_\parallel \frac{\omega^2}{c^2} + k_x^2 \frac{\epsilon_\parallel}{\epsilon_\perp}, \quad q_\perp^2 = \boldsymbol{k}_\perp^2 - \epsilon_\perp \frac{\omega^2}{c^2} + k_x^2. \tag{12}$$

The solutions (10) and (11), along with $E_z(x)$ which is not reported here as it will not be required in the following sections, refer to bulk excitations [22] of the electromagnetic field in an infinite medium and comprise both longitudinal and transverse waves.

III. THE ENERGY LOSS

In this section we derive the energy lost by the moving charge. This is calculated within a thin layer of an infinite medium and for a particle velocity directed at an arbitrary angle with respect to the optical c axis. We find it convenient here to take a system of coordinates [23] whereby the wave vector $\boldsymbol{k}$ of the excited bulk mode is characterized by the polar and azimuthal angles χ and φ with the polar axis directed along the optical c axis as shown in Fig. 1.

The energy W lost by the charge can be evaluated [5] as the work done by the electric field [24] on the charge moving within a layer of volume V_{layer} and thickness L, i.e.,

$$W = -\int_{V_{layer}} d\boldsymbol{r} \int_{-\infty}^{\infty} dt\, \mathrm{Re}[\mathbf{J}(\mathbf{r},t)] \cdot \mathrm{Re}[\mathbf{E}(\mathbf{r},t)]$$

$$= -\frac{q_e}{(2\pi)^3}\,\mathrm{Re}\int d\boldsymbol{k}_\perp \int_{-\infty}^{\infty} d\omega \int_{-L/2}^{L/2} dx\, \frac{\boldsymbol{v}}{v_x} \cdot \boldsymbol{E}_{\boldsymbol{k}_\perp,\omega}(x) e^{-ik_x x}. \tag{13}$$

Upon inserting Eqs. (10) and (11) into Eq. (13) and using the property

$$q_\parallel^2 = \frac{\epsilon_\parallel}{\epsilon_\perp}\boldsymbol{q}_\perp^2 - \epsilon_r \boldsymbol{k}_\perp^2, \tag{14}$$

the probability that the charge loses energy subsequent to the excitation of a mode of frequency ω and wave vector $\boldsymbol{k}$ can be written after some algebra in the form

$$\frac{dW}{d\omega d\boldsymbol{k}_\perp} = \frac{q_e^2 \omega L}{2\pi^2 v_x^2}\,\mathrm{Im}\left\{\frac{1}{\epsilon_\perp q_\parallel^2} - \frac{v^2}{c^2 q_\parallel^2}\left[1 + \epsilon_r \times \left(1 - \frac{k_z^2}{q_\perp^2}\right)\sin^2\theta\right]\right\}, \tag{15}$$

where

$$k_z = k_\perp \cos\varphi = k \sin\chi \cos\varphi \tag{16}$$

and $\boldsymbol{k}_\perp$ are, respectively, the projections of $\boldsymbol{k}$ along the z axis and on the principal plane. The second term in the square brackets depends both on the reduced dielectric tensor ϵ_r and on the angle θ between the charge velocity and the optical c axis. Such a term is therefore absent either for an isotropic medium ($\epsilon_\parallel = \epsilon_\perp$) or for a charge moving along the optical c axis ($\theta = 0$). When incidence does not occur along the optical c axis ($\theta \neq 0$) the θ dependent term in Eq. (15) may, however, cause appreciable modifications of the loss spectrum.

In the limit $\beta \to 0$ the rate (15) reduces to the nonrelativistic energy-loss function for uniaxial [25] media, i.e.,

$$\frac{dW_{NR}}{d\omega d\boldsymbol{k}_\perp} = \frac{q_e^2 L}{2\pi^2 \omega \cos^2\theta}\mathcal{S}^2(\chi,\varphi,\theta)\,\mathrm{Im}\left\{\frac{1}{\epsilon_\perp(1 + \epsilon_r \cos^2\chi)}\right\}, \tag{17}$$

where we introduce the function $\mathcal{S}$,

$$\mathcal{S}^2(\chi,\varphi,\theta) = \left(\frac{\omega}{kv}\right)^2 = (\cos\theta\cos\chi + \sin\theta\sin\chi\sin\varphi)^2 = \cos^2\gamma, \tag{18}$$

denoting the projection of the bulk mode wave vector $\boldsymbol{k}$ along the direction of the particle velocity $\boldsymbol{v}$. Pronounced

maxima in Eq. (17) occur for vanishing values of the denominator of the imaginary part and correspond to losses due to the excitation of longitudinal modes, i.e., plasmon losses [26]. In particular, the interpretation of early experiments on electron energy loss in anisotropic graphite [27] was just based [28,29] on this result.

With the help of Eqs. (14) and (8), we can rewrite the differential energy-loss function (15) as

$$\frac{dW}{d\omega d\boldsymbol{k}_\perp}=\frac{q_e^2\beta^2 v^2 L}{2\pi^2\omega v_x^2}\mathcal{S}^2\times\mathrm{Im}\left\{\frac{1-(\beta^2\epsilon_\perp)^{-1}+\epsilon_r\sin^2\theta(1-\beta^2\epsilon_\perp\mathcal{S}^2-\sin^2\chi\cos^2\varphi)\mathcal{D}_o^{-1}}{\mathcal{D}_{eo}}\right\}, \tag{19}$$

where $\mathcal{D}_o=1-\beta^2\epsilon_\perp\mathcal{S}^2$ and $\mathcal{D}_{eo}=1-\beta^2\epsilon_\parallel\mathcal{S}^2+\epsilon_r\cos^2\chi$ with the function $\mathcal{S}$ defined in (18) and as usual $\beta=v/c$. Maxima of this function occur at the poles of the imaginary part of Eq. (19). Apart from the plasmon pole contribution [30] already discussed in Eq. (17), it is possible to show, by carrying out the imaginary part on the right hand side of Eq. (19), that the two other denominators, $\mathcal{D}_o$ and $\mathcal{D}_{eo}$, yield two distinct pole conditions that correspond instead to losses due to the excitation of transverse modes, i.e., Cherenkov losses.

In the absence of the external field, the imaginary part of the dielectric function of cuprous oxide (Cu_2O), the sample material that we will examine below, is in general quite smaller than its real part for frequencies around the medium resonances [31,32] while the imaginary parts of the two tensor components $\epsilon_\parallel$ and $\epsilon_\perp$ turn out to be even smaller than the corresponding real parts when the external field is on [33]. The medium can be shown to exhibit in this case large degrees of transparency at resonance [33] so that Cherenkov emission will not be substantially hampered by absorption. To a good approximation, resonant Cherenkov emission in the presence of the external field can then be thought to occur in a nearly transparent regime so that strongest Cherenkov emission would occur at the maxima of the Cherenkov energy loss in Eq. (19).

We now proceed to discuss Cherenkov emission within this approximation so that, in the limit in which the imaginary parts of the relevant dielectric tensor can be neglected, one obtains from the vanishing of the denominator of Eq. (19) the two coherence conditions in the form ($\chi,\gamma\neq\pi/2$)

$$1-\beta^2\epsilon_\perp\cos^2\gamma\simeq 0 \tag{20}$$

and

$$1-\beta^2\epsilon_\parallel\cos^2\gamma+\epsilon_r\cos^2\chi\simeq 0. \tag{21}$$

Because the propagation of emitted ordinary waves is characterized only by $\epsilon_\perp$ and that of extraordinary waves by both $\epsilon_\perp$ and $\epsilon_\parallel$ dielectric functions [20], it follows that Eqs. (20) and (21) yield, respectively, the conditions for the emission of *ordinary* and *extraordinary* waves in the process of Cherenkov emission. Notice that the condition (20) no longer exists at *normal incidence* ($\theta=0$) in which case only extraordinary waves can propagate whereas at *oblique incidence* ($\theta\neq 0$) ordinary and extraordinary waves can both propagate. Oblique incidence does not simply change the effective thickness traversed by the particle but it gives rise to a new type of volume excitation.

A. Cherenkov ordinary waves

Coherence conditions determine the angle of the cone over which Cherenkov radiation is emitted and for ordinary waves this is obtained by solving Eq. (20) for γ at a given wave frequency and particle speed. By further requiring that $\cos^2\gamma$ be real and less than unity we obtain the threshold condition,

$$\beta^2\geqslant\beta_c^{o2}=\frac{1}{\epsilon_\perp}, \tag{22}$$

where $\beta_c^o=v_c^o/c$ determines the critical velocity for emission of Cherenkov ordinary waves determined by setting $\gamma=0$. For a particle moving at the critical velocity v_c^o, ordinary Cherenkov radiation is emitted in the direction $\boldsymbol{k}$ along $\boldsymbol{v}$ which is then the Cherenkov cone axis. For a particle moving with velocity in the *x-y* plane the emitted ordinary Cherenkov wave has the same geometrical properties as the one emitted in an isotropic medium of dielectric function $\epsilon_\perp$.

B. Cherenkov extraordinary waves

For a given velocity direction θ the cone over which extraordinary radiation is emitted is now determined both by χ and γ satisfying the condition (21) and hence in this case emission occurs over conical surfaces that are, in general, noncircular. Such surfaces are symmetric with respect to the *x-y* plane so that for a particle moving at critical velocity extraordinary waves are emitted in the direction $\boldsymbol{k}_e$ at an angle χ_e different from θ (cf. Fig. 1) and given by

$$\tan\chi_e=\frac{\epsilon_\parallel}{\epsilon_\perp}\tan\theta. \tag{23}$$

This result can be obtained by minimizing β given in Eq. (21) under the assumption that both $\epsilon_\parallel$ and $\epsilon_\perp$ are positive. It is worth noting that when both of them are negative the coherence condition cannot be satisfied, whereas if either one of them is negative it can be satisfied even for a negligible β at an angle χ_o given by $\tan\chi_o=\sqrt{-\epsilon_\parallel/\epsilon_\perp}$, independent of θ and corresponding to the nonrelativistic pole of Eq. (17). At the critical speed the coherence condition (21) becomes

$$1-\beta_c^{e2}\epsilon_\parallel\cos^2(\theta-\chi_e)+\epsilon_r\cos^2\chi_e\simeq 0, \tag{24}$$

so that upon eliminating χ_e from Eqs. (23) and (24) the threshold condition for extraordinary waves takes on the form

$$\beta^2 \geqslant \beta_c^{e2} = \frac{1}{\epsilon_\perp} \frac{1}{1+\epsilon_r \sin^2\theta}. \tag{25}$$

The angular term on the right hand side of Eq. (25) is the oblique incidence contribution to the critical speed for emission of extraordinary Cherenkov waves and reduces to unity as $\theta \to 0$. Appreciable reductions of the threshold condition are then expected to occur for large and positive values of the reduced dielectric function ϵ_r and for oblique rather than normal incidence. Both conditions (22) and (25) further reduce to the Cherenkov threshold condition $\beta^2 \epsilon > 1$ for an isotropic medium [5].

The integrated energy loss spectrum can be obtained from the differential loss (15) and that is,

$$\frac{dW}{d\omega} = \frac{q_e^2 \omega L'}{2\pi^2 v} \int d^3k \, \delta(\boldsymbol{k}\cdot\boldsymbol{v}-\omega) \mathrm{Im}\left\{ \frac{1}{\epsilon_\perp q_\parallel^2} - \frac{\beta^2}{q_\parallel^2}\left[1+\epsilon_r\left(1-\frac{k_z^2}{q_\perp^2}\right)\sin^2\theta \right] \right\}, \tag{26}$$

where L' is the thickness traversed by the particle along its path. The expression (26) also applies to the case of a particle moving perpendicular to the optical c axis ($\theta = \pi/2$) in which case it can be shown to agree with the result (B7) derived separately in Appendix B.

Ordinary and extraordinary Cherenkov waves see different refractive indexes and can simultaneously be emitted as the charge traverses the medium. Ordinary waves are emitted with uniform intensity distributed over circular cones whose generatrices make an angle γ about the direction of $\boldsymbol{v}$ which is determined for a given speed and wave frequency by the condition (20). Extraordinary waves are instead emitted, in general, with a nonuniform intensity distribution and over noncircular cones with generatrices determined by the set of angles $\{\gamma, \chi\}$ about $\boldsymbol{k}_e$ through Eq. (21).

IV. RESONANT EMISSION ENHANCEMENT IN DRIVEN Cu_2O

It follows from the above analysis that Cherenkov emission occurs in correspondence to the maxima of Eq. (19) subject to the coherence conditions (20) and (21) and threshold conditions (22) and (25).

We here investigate the possibility of increasing the resonant yield of Cherenkov light in a crystal of cuprous oxide (Cu_2O) when this is coherently driven by an external light beam. Cuprous oxide exhibits exciton resonances and we will examine, in particular, Cherenkov emission at frequencies ω close to the $2P$ "yellow" exciton line [31,32] when the external beam of frequency ω_c is tuned to the $2P$ to $1S$ exciton transition of frequency $\omega_{2P}-\omega_{1S}$ [33–35]. The external light beam and the emitted Cherenkov light coupling the $2P$ state, respectively, to the $1S$ and to the ground states realize a Λ configuration leading to a narrow transparency window for Cherenkov light emitted at about the $2P$ exciton line, justifying the treatment of Cherenkov emission in a nonabsorbing regime adopted in the preceding section. Transparency occurs for an external beam Rabi frequency Ω larger than or of the order of $\sqrt{\gamma_{1S}\gamma_{2P}}$ [33], where γ_{1S} and γ_{2P} are the linewidths of the dipole forbidden $1S$ state and of the second class allowed $2P$ state.

From the Λ-type model Hamiltonian describing such a coherently driven system we can calculate the dressed medium dielectric tensor that turns out to depend [36] on the external beam polarization as well as on the detailed structure of the exciton levels. The external beam reduces, in fact, the cubic symmetry of Cu_2O so that the form of the dielectric tensor will depend on the orientation of the external beam polarization with respect to the cubic axes $\hat{e}_x$, $\hat{e}_y$, and $\hat{e}_z$. For an external beam linearly polarized along [1,0,0], e.g., the system is reduced to a uniaxial crystal having $\hat{e}_x$ as optical axis and similarly for an external beam polarized along $\hat{e}_y$ or $\hat{e}_z$ [37]. For a polarization along the diagonal [1,1,1], the system is reduced to a uniaxial crystal having [1,1,1] as optical axis and likewise for polarizations along the other two main diagonals. The form of the dielectric tensor further depends on the specific exciton levels; this is treated extensively in Ref. [36] and will not be discussed here.

We now proceed to discuss the enhancement of resonant Cherenkov emission for a specific configuration in which the external beam is polarized either along [1,0,0] or along the main cubic diagonal [1,1,1] while the $2P$ (Γ_4^-) states are well separated from the other states of the $2P$ manifold [36]. The external beam instead resonantly couples the $1S$ (Γ_5^+) and the $2P$ (Γ_4^-) exciton levels [36]. Cubic, principal, and optical axes for the two external beam configurations that we consider here are shown in Fig. 1

For an external beam polarized along [1,0,0], the dressed dielectric tensor can be shown to be uniaxial [33,36] with respect to the principal axes $\hat{e}_1=[1,0,0]$, $\hat{e}_2=[0,1,0]$, and $\hat{e}_3=[0,0,1]$ with optical c axis directed along [1,0,0],

$$\epsilon_{11}=\epsilon_\parallel, \quad \epsilon_{22}=\epsilon_{33}=\epsilon_\perp, \quad \epsilon_{j\neq k}=0. \tag{27}$$

Here

$$\epsilon_\perp = \epsilon(\Omega) \equiv \epsilon_\infty + \frac{A\,\gamma_{2P}(\omega_c-\omega+\omega_{1S}-i\gamma_{1S})}{(\omega_{2P}-\omega-i\gamma_{2P})(\omega_c-\omega+\omega_{1S}-i\gamma_{1S})-\Omega^2/4}, \tag{28}$$

where $\epsilon_{\|}$ is obtained by setting $\Omega \to 0$ in the above equation while $\epsilon_{\infty} \simeq 6.5 + i\, 2 \times 10^{-3}$ denotes the background dielectric constant. For the yellow exciton series of bulk Cu_2O one has $\hbar\omega_{2P} \simeq 2.148$ eV and $\hbar\omega_{1S} \simeq 2.033$ eV for the energy of the levels and $\hbar\gamma_{2P} \simeq 1$ meV [34,35] and $\hbar\gamma_{1S} \simeq 0.05$–$0.1$ meV [34,35] for the corresponding linewidths. From the measured values of γ_{2P} [34,35] and of the oscillator strength [38,39] the coefficient A can be estimated to be $A \simeq 0.02$ [33]. The external beam Rabi frequency Ω is proportional to the $1S$-$2P$ transition dipole matrix element D_{21} and to the external electric field amplitude [33,36].

For an external beam along [1,1,1], on the other hand, the dielectric tensor is uniaxial with respect to the principal axes $\hat{e}_1 = [1,1,1]/\sqrt{3}$, $\hat{e}_2 = [1,-1,0]/\sqrt{2}$, and $\hat{e}_3 = [1,1,-2]/\sqrt{6}$ with the optical c axis directed along [1,1,1], i.e.,

$$\epsilon_{11} = \epsilon_{\|} = \epsilon\left(\Omega \propto \sqrt{\frac{2}{3}} D_{21}\right),$$

$$\epsilon_{22} = \epsilon_{33} = \epsilon_{\perp} = \epsilon\left(\Omega \propto \sqrt{\frac{1}{6}} D_{21}\right), \tag{29}$$

with $\epsilon_{j \neq k} = 0$ and where the form of $\epsilon(\Omega)$ is given in Eq. (28). Note that the expression for Ω is scaled with appropriate numerical factors shown in Eq. (29) with respect to the one in Eq. (28). Unlike in the case of an external beam polarized along [1,0,0], the principal axes $\hat{e}_1$, $\hat{e}_2$, and $\hat{e}_3$ are not parallel to the crystal cubic axes as shown in Fig. 1.

The substitution of the tensor (27) along with Eq. (7) into Eqs. (19) and (21) gives, respectively, the charge energy loss and the coherence condition associated with the emission of Cherenkov *extraordinary waves*. Likewise when the tensor (29), representing the other beam configuration, is used.

The coherence condition (21) for resonant emission in the [1,0,0] configuration is reported, e.g., in Fig. 2 for polar and azimuthal angles $\{\chi, \varphi\}$ spanning an octant of the scattering solid angle and various degrees of oblique incidence including the limit case of incidence that is parallel and nearly perpendicular to the optical c axis. Apart from the case of a charged particle moving parallel to the optical axis, in which no dependence on the azimuthal angle φ is exhibited, the coherence condition (21) depends on φ and hence at oblique incidence Cherenkov emission occurs over conical surfaces that are, in general, noncircular [4]. For a given angle of incidence θ, each pair of angles $\{\chi, \varphi\}$ defines in fact a generatrix of the surface and it further follows from Eq. (19) that the emitted intensity is different on different generatrices, i.e., the radiated intensity is not uniform over the Cherenkov conical surface.

We compare instead in Fig. 3 the differential loss (19) around the resonance region for both [1,0,0] and [1,1,1] configurations. The external field intensity, the incident particle geometry, and the scattered wave direction set by the condition (21), are held fixed for each configuration. In this region plasmon poles in the numerator of Eq. (19) are absent and the large Cherenkov losses that are observed anticipate a considerable enhancement of the Cherenkov emission within this region. This is seen to arise only in the presence of the field and to depend, in particular, on the direction of the field orientation with respect to the crystal cubic axes and to the incident charged particle direction. In the [1,0,0] configuration, in fact, large enhancements are only observed for a field not polarized along the direction of $\boldsymbol{v}$ (oblique incidence) whereas in the other configuration enhancements of comparable magnitudes are instead observed regardless of whether the field is polarized along (normal incidence [40]) or not along $\boldsymbol{v}$. Depending upon the field configuration the largest emission yields in the presence of the field turn out to be 100 to 150 times that obtained when the external beam is instead switched off.

Larger yields could be obtained with stronger external fields that would, in turn, allow one to observe larger yields

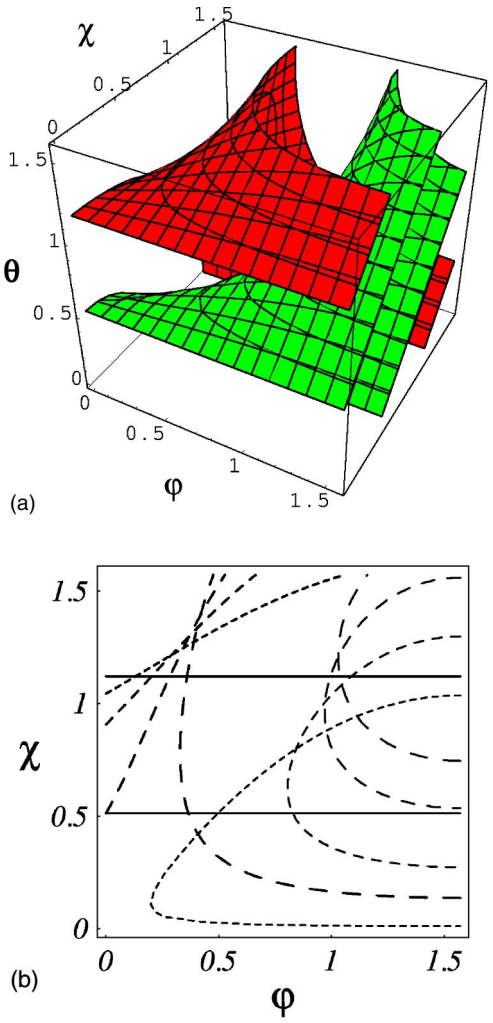

FIG. 2. (Upper frame) Cherenkov coherence condition (21) for two different velocities $v = 0.9c$ (outer red surface) and $v = 0.45c$ (inner green surface). Resonant radiation is only emitted for angles of incidence (θ) and wave vector orientations $\{\chi, \varphi\}$ lying on these surfaces. (Lower frame) Horizontal section for $\theta = 0$, 30°, 58°, and 86° for $v = 0.9c$ (black) and for $v = 0.45c$ (gray). Increasing angles of incidence correspond to increasing dash lengths. The straight line corresponds to normal incidence ($\theta = 0$) in which case light is emitted over a circular cone making a fixed angle χ_o about the optical axis and determined by the intercept with the vertical χ axis.

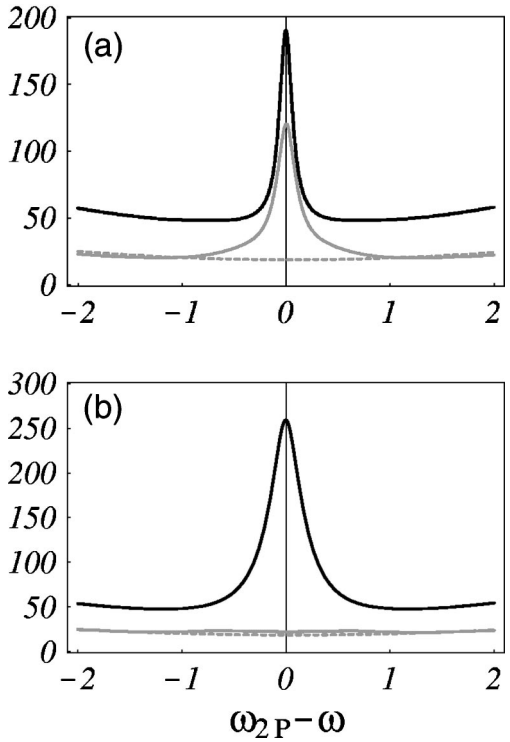

FIG. 3. Differential energy loss (19) in units of $q_e^2/\omega_{2P}L$ in the absence (dashed curve) and in the presence (solid curve) of the external field vs the frequency ω that is measured with respect the exciton resonance frequency ω_{2P} with $\hbar\omega_{2P}=2147$ meV. The field with Rabi frequency $\Omega=2$ is polarized along the main cubic diagonal [1,1,1] (upper frame) and along [1,0,0] (lower frame). All frequencies are in units of γ_{2P}, with $\hbar\gamma_{2P}=1$ meV. The particle impinges with velocity $v=0.9c$ at an angle $\theta\simeq 80°$ while $\{\chi,\varphi\}\simeq\{17°,58°\}$ (upper frame) and $\{\chi,\varphi\}\simeq\{18°,56°\}$ (lower frame) denote directions corresponding to a local maximum of the loss (19). Gray curves, multiplied by a factor f 10 to allow for comparison, correspond to the case of normal incidence ($\theta=0$) for a maximum loss occurring in the direction $\chi\simeq 64°$.

over a wider range of frequencies in the resonance region. Both effects are shown in Fig. 4 for a fixed incident particle geometry and scattered wave direction in the [1,0,0] configuration. Similar results hold essentially unchanged for the other [1,1,1] configuration and hence will not be discussed here. Note that the largest value of Ω used in Fig. 4 corresponds to an electric field amplitude $E\simeq$ 25 KV/cm which is well within the range of intensities used in common experiments with Cu_2O [41].

The discussion on the coherence condition (20) for the resonant emission of *ordinary waves* can be carried out in much the same way as done for the extraordinary waves counterpart. This leads to quantitatively similar results: in Eq. (21) the reduced tensor ϵ_r, which determines the strength of the medium induced anisotropy, turns out to be small in fact for coherently driven Cu_2O [42] owing to the fact that this material exhibits a weak $2P$ exciton transition with a concomitant fairly large bulk dielectric constant [31,32,43]. Because of such a weak anisotropy it follows directly from Eqs. (20), (21), and (23) that the two conical surfaces over which ordinary and extraordinary Cherenkov

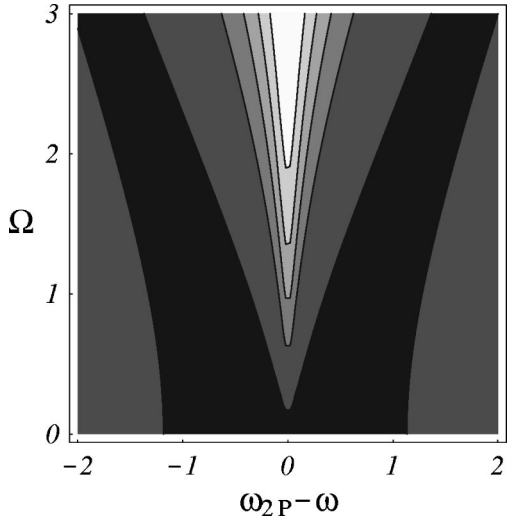

FIG. 4. Differential loss contour profiles at 50, 100, 150, 200, and 250 for an external field of variable intensity and polarized along [1,0,0]. Units, particle and field parameters are the same as in Fig. 3. The darkest area corresponds to the smallest loss while increasingly lighter areas correspond to increasing losses.

waves are emitted will be nearly overlapping though the two different types of waves may still be distinguished from one another as they differ in their electric field polarizations $\boldsymbol{e}^o$ and $\boldsymbol{e}^e$. These are given in their general form in Appendix C.

V. SUMMARY AND CONCLUSIONS

The Vavilov-Cherenkov effect has been studied extensively ever since its discovery [1–3]. Mainly because most part of the applications refer to high-energy detector materials for which dispersion and absorption may, in general, not be important [4], Cherenkov emission is usually referred to as occurring in nondispersive transparent media and hence only little attention has been devoted to the emission in other materials.

In the present work we show that for a certain class of dispersive and absorbing solid media the Cherenkov effect can be largely modified by the presence of an external electromagnetic field [44]. As an illustrative example we study such modifications in the absorbing region of the $2P$ ''yellow'' exciton resonance in Cu_2O in the presence of an external field that is resonant with the $1S-2P$ transition. Our numerical estimates anticipate a large increase of the resonant Cherenkov emission yield. This is shown to depend on the external electric field strength and orientation, with respect to the medium cubic axes and to the incident charged particle direction, which induce changes in the complex tensor components of the dielectric function and in the geometrical factors both contained in the differential loss function (19). The resonant emission yield can then be controlled directly by varying the intensity and orientation of the external field so that fairly small enhancements taking place for a sufficiently intense field polarized both along $\boldsymbol{v}$ and along the medium cubic axes are seen to alternate with very large ones that can instead be attained when the field is not polarized in the $\boldsymbol{v}$ direction.

In particular, we have provided in Secs. II and III a detailed analysis of the Vavilov-Cherenkov effect in a dispersive and resonant absorbing uniaxial medium, as required by the presence of the external field, with inclusion of the case of a particle impinging off the optical axis. The results of these sections extend those developed for the Cherenkov emission in nondispersive and transparent uniaxial crystals for particles moving both parallel and perpendicular to the optical axis [45].

ACKNOWLEDGMENTS

We are grateful to F. Pegoraro, E. Arimondo, and M. Giuntini for enlightening discussions and we greatly acknowledge support by the INFM (Project PRA ''Photon-Matter'') and the European Community (Contract No. HPRICT1999-00111).

APPENDIX A

The electromagnetic field radiated by a fast charge in an anisotropic nonmagnetic medium ($\mu=1$) is described by the Maxwell's equations

$$\boldsymbol{\nabla}\cdot\mathbf{E}(\mathbf{r},t)=-\frac{\partial\mathbf{B}(\mathbf{r},t)}{c\,\partial t},\quad \boldsymbol{\nabla}\cdot\mathbf{H}(\mathbf{r},t)=\frac{\partial\mathbf{D}(\mathbf{r},t)}{c\,\partial t}+\frac{4\pi\mathbf{J}(\mathbf{r},t)}{c}, \tag{A1}$$

$$\boldsymbol{\nabla}\cdot\mathbf{D}(\mathbf{r},t)=4\pi\rho(\mathbf{r},t),\quad \boldsymbol{\nabla}\cdot\mathbf{B}(\mathbf{r},t)=0, \tag{A2}$$

with the (free) charge and (free) current densities given by Eqs. (2) and (3), respectively. If x, y, and z denote the medium *principal axes* the dielectric tensor is diagonal along this set of axes, i.e.,

$$\boldsymbol{\epsilon}_{\omega}=\begin{pmatrix}\epsilon_{xx,\omega} & 0 & 0\\ 0 & \epsilon_{yy,\omega} & 0\\ 0 & 0 & \epsilon_{zz,\omega}\end{pmatrix}. \tag{A3}$$

In particular, for an uniaxial medium with optical c axis along x the displacement Fourier transverse components are

$$D_{\mathbf{k}_\perp,\omega}(x)\big|_x=\epsilon_{\parallel,\omega}E_{\mathbf{k}_\perp,\omega}(x)\big|_x,\quad D_{\mathbf{k}_\perp,\omega}(x)\big|_{y,z}=\epsilon_{\perp,\omega}E_{\mathbf{k}_\perp,\omega}(x)\big|_{y,z}, \tag{A4}$$

where we set

$$\epsilon_{xx,\omega}=\epsilon_{\parallel,\omega},\quad \epsilon_{yy,\omega}=\epsilon_{zz,\omega}=\epsilon_{\perp,\omega}. \tag{A5}$$

Using the same expansion procedure (1) and with the help of Eq. (2) we expand both sides of the first equation in Eq. (A2) so that using Eq. (A3) we obtain

$$\frac{\partial E_{\mathbf{k}_\perp,\omega}(x)\big|_x}{\partial x}=\frac{4\pi\rho_{\mathbf{k}_\perp,\omega}(x)}{\epsilon_{\parallel,\omega}}-\frac{i\,\epsilon_{\perp,\omega}}{\epsilon_{\parallel,\omega}}[k_yE_{\mathbf{k}_\perp,\omega}(x)\big|_y+k_zE_{\mathbf{k}_\perp,\omega}(x)\big|_z,], \tag{A6}$$

which gives the variation of the electric field component along the optical c axis. The transverse Fourier component of the charge density (2) on the right hand side of Eq. (A6) is obtained in a similar manner, i.e.,

$$\rho_{\mathbf{k}_\perp,\omega}(x)=\frac{q_e}{v_x}\exp\left\{i\,x\,\frac{\omega-k_yv_y}{v_x}\right\}\equiv\frac{q_e}{v_x}e^{ixk_x}\left(k_x=\frac{\omega-k_yv_y}{v_x}\right), \tag{A7}$$

whereas

$$\mathbf{J}_{\mathbf{k}_\perp,\omega}(x)=\boldsymbol{v}\frac{q_e}{v_x}e^{i\,x\,k_x}. \tag{A8}$$

We can now combine the first two equations in Eq. (A1) to get the following wave equation:

$$\vec{\boldsymbol{\nabla}}[\vec{\boldsymbol{\nabla}}\cdot\mathbf{E}(\mathbf{r},t)]-\boldsymbol{\nabla}^2\mathbf{E}(\mathbf{r},t)+\frac{\partial^2\mathbf{D}(\mathbf{r},t)}{c^2\partial t^2}=-\frac{4\pi}{c^2}\frac{\partial\mathbf{J}(\mathbf{r},t)}{\partial t}. \tag{A9}$$

By first expanding $\mathbf{E}(\mathbf{r},t)$, $\mathbf{D}(\mathbf{r},t)$, and $\mathbf{J}(\mathbf{r},t)$ according to Eq. (1) and then using Eq. (A6) to eliminate in each of the three components of the gradient on the left hand side of Eq. (A9) spatial variations of the electric field not occurring along the optical c axis where, for instance, one has for the x component

$$\vec{\boldsymbol{\nabla}}[\vec{\boldsymbol{\nabla}}\cdot\mathbf{E}(\mathbf{r},t)]\big|_x=\frac{1}{(2\pi)^3}\int d\mathbf{k}_\perp\int d\omega\,e^{i\mathbf{k}_\perp\cdot\mathbf{r}-i\omega t}\left(\frac{4\pi}{\epsilon_{\perp,\omega}}\frac{\partial\rho_{\mathbf{k}_\perp,\omega}(x)}{\partial x}-\epsilon_{r,\omega}\frac{\partial^2E_{\mathbf{k}_\perp,\omega}(x)}{\partial x^2}\right), \tag{A10}$$

we obtain with the help of Eqs. (A4), (A7), and (A8) the wave equations (4), (5), and (6).

APPENDIX B

For completeness, we discuss here the specific case of a particle moving perpendicular to the optical c axis ($v_x=0$). This case has to be considered separately because the expressions for the electric field, Eqs. (10) and (11), obtained in Sec. II as well as the energy loss (15) do not admit simple limits as $\theta\to\pi/2$. In place of Eq. (1), it is convenient to write the electric field as

$$\mathbf{E}(\mathbf{r},t)=\frac{1}{(2\pi)^3}\int\int dk_xdk_z\int d\omega\,e^{ik_xx+ik_zz-i\omega t}\boldsymbol{E}_{\mathbf{k}_{x,z},\omega}(y), \tag{B1}$$

so that using the same approach of Appendix A, one arrives at the following Maxwell equations:

$$\left(\frac{\epsilon_\parallel}{\epsilon_\perp}k_x^2-\partial_y^2+k_z^2-\epsilon_\parallel\frac{\omega^2}{c^2}\right)E_x(y)=-\frac{4\pi i q_e k_x}{v\epsilon_\perp}e^{ik_y y}, \tag{B2}$$

$$\left(-\partial_y^2-\epsilon_\perp\frac{\omega^2}{c^2}+k_x^2+k_z^2\right)E_y(y)$$

$$=ik_x\epsilon_r\partial_y E_x(y)-4\pi i q_e\left(\frac{k_y}{v\epsilon_\perp}-\frac{\omega}{c^2}\right)e^{ik_y y}, \tag{B3}$$

$$\left(-\partial_y^2-\epsilon_\perp\frac{\omega^2}{c^2}+k_x^2+k_z^2\right)E_z(y)$$

$$=-k_z k_x\epsilon_r E_x(y)-\frac{4\pi i q_e k_z}{v\epsilon_\perp}e^{ik_y y}, \tag{B4}$$

where $k_y=\omega/v$ and again with the shorthand notation $E_{\{x,y,z\}}(y)=E_{\mathbf{k}_{x,z,\omega}}(y)|_{\{x,y,z\}}$.

Such equations can be solved and one obtains for the electric field $E_y(y)$, the only component needed in this case to calculate the energy loss,

$$E_y(y)=-\frac{4\pi i q_e\omega}{\epsilon_\perp v^2 q_\perp^2}e^{i(\omega/v)y}\left[1-\epsilon_\perp\frac{v^2}{c^2}-\epsilon_r\frac{k_x^2}{q_\parallel^2}\right], \tag{B5}$$

where, similarly to Eq. (12), one has

$$q_\parallel^2=\frac{\omega^2}{v^2}+k_z^2-\epsilon_\parallel\frac{\omega^2}{c^2}+k_x^2\frac{\epsilon_\parallel}{\epsilon_\perp},\quad q_\perp^2=\frac{\omega^2}{v^2}+k_z^2-\epsilon_\perp\frac{\omega^2}{c^2}+k_x^2. \tag{B6}$$

The differential loss function takes now the form

$$\frac{dW}{d\omega d\mathbf{k}_{xz}}=\frac{q_e^2\omega L'}{2\pi^2 v^2}Im\left\{\frac{1}{\epsilon_\perp q_\perp^2}-\frac{\beta^2}{q_\perp^2}-\frac{\epsilon_r k_x^2}{\epsilon_\perp q_\perp^2 q_\parallel^2}\right\}, \tag{B7}$$

where L' is here the length of the sample traversed by the particle in the $\hat{y}$ direction and whose poles lead to the coherence conditions [47]

$$1-\beta^2\epsilon_\perp\sin^2\chi\sin^2\varphi\simeq 0 \tag{B8}$$

and

$$1-\beta^2\epsilon_\parallel\sin^2\chi\sin^2\varphi+\epsilon_r\cos^2\chi\simeq 0. \tag{B9}$$

As for those obtained in Eqs. (20) and (21), these correspond to the conditions for the emission of ordinary and extraordinary Cherenkov waves, respectively, and again recover known results for a particle moving perpendicular to the optic *c* axis in a nonabsorbing medium [4].

APPENDIX C

We give here the explicit form of the electric $\boldsymbol{e}^{o,e}$ and displacement $\boldsymbol{d}^{o,e}$ field *polarizations* for either ordinary or extraordinary waves. If $\boldsymbol{n}$ is the unit vector in the direction of the radiated wave vector $\boldsymbol{k}$, one has from the general properties of plane waves in a uniaxial medium [46]

$$\boldsymbol{d}^{o,e}\cdot\boldsymbol{n}=0, \tag{C1}$$

$$\boldsymbol{d}^{o}\cdot\boldsymbol{d}^{e}=0, \tag{C2}$$

while a relation analogous to Eq. (A4) holds for the corresponding unit vectors.

Ordinary wave polarization. It follows directly from Eq. (C1) that

$$n_x^2+n_y^2+n_z^2=1,$$

$$d_x^{o2}+d_y^{o2}+d_z^{o2}=1,$$

$$d_x^o n_x+d_y^o n_y+d_z^o n_z=0, \tag{C3}$$

so that taking advantage of the fact that for ordinary waves the displacement vector is perpendicular to the optical *c* axis, we can solve this system of equations to obtain

$$d_x^o=0,\quad d_y^o=\frac{n_z}{\sqrt{1-n_x^2}},\quad d_z^o=-\frac{n_y}{\sqrt{1-n_x^2}}. \tag{C4}$$

These can in turn be used to obtain the electric field polarization components upon inverting Eq. (A4), namely [47],

$$\mathbf{e}^o\simeq\frac{n_z}{\epsilon_\perp\sqrt{1-n_x^2}}\hat{\mathbf{y}}-\frac{n_y}{\epsilon_\perp\sqrt{1-n_x^2}}\hat{\mathbf{z}} \tag{C5}$$

and hence

$$\mathbf{d}^o\simeq\frac{1}{\epsilon_\perp}\mathbf{e}^o. \tag{C6}$$

Extraordinary wave polarization. The polarizations are in this case obtained by solving a system of equations similar to Eq. (C3) and by further using the property (C2). One obtains for the displacement field polarization components

$$d_x^e=\sqrt{1-n_x^2},\quad d_y^e=-\frac{n_x n_y}{\sqrt{1-n_x^2}},\quad d_z^e=-\frac{n_x n_z}{\sqrt{1-n_x^2}} \tag{C7}$$

and again by inverting Eq. (A4) one gets [47]

$$\mathbf{e}^e\simeq\frac{\sqrt{1-n_x^2}}{\epsilon_\parallel}\hat{\mathbf{x}}-\frac{n_x n_y}{\epsilon_\perp\sqrt{1-n_x^2}}\hat{\mathbf{y}}-\frac{n_x n_z}{\epsilon_\perp\sqrt{1-n_x^2}}\hat{\mathbf{z}}, \tag{C8}$$

and hence

$$\mathbf{d}^e\simeq\sqrt{1-n_x^2}\hat{\mathbf{x}}-\frac{n_x n_y}{\sqrt{1-n_x^2}}\hat{\mathbf{y}}-\frac{n_x n_z}{\sqrt{1-n_x^2}}\hat{\mathbf{z}}. \tag{C9}$$

Note that the electric and displacement field polarizations are not parallel to one another which implies that *wave* and *ray* vectors, perpendicular to $\mathbf{d}^e$ and to $\mathbf{d}^e$, respectively [46], are in general not along the same direction for extraordinary waves.

[1] S. Vavilov, Dokl. Akad. Nauk SSSR **2**, 457 (1934).
[2] P.A. Cherenkov, Dokl. Akad. Nauk SSSR **2**, 451 (1934).
[3] I. Frank and I. Tamm, Dokl. Akad. Nauk SSSR **14**, 107 (1937).
[4] J. Jelley, *Cherenkov Radiation* (Pergamon Press, Oxford, 1958), Sec. 3.3.
[5] L.D. Landau and E.M. Lifschitz, *Electrodynamics of Continuous Media* (Pergamon Press, Oxford, 1960), Sec. 86.
[6] H. Abarbanel, M. Rabinovich, and M. Sushchik, *Introduction to Non-Linear Dynamics for Physicists* (World Scientific, Singapore, 1993).
[7] P. Budini, Nuovo Cimento **10**, 237 (1953).
[8] A. Cripsin and G. Fowler, Rev. Mod. Phys. **42**, 290 (1970).
[9] S. Ahlen, Rev. Mod. Phys. **52**, 121 (1980).
[10] U. Fano, Phys. Rev. **103**, 1202 (1956).
[11] E. Fermi, Phys. Rev. **57**, 485 (1940).
[12] I. Tamm, J. Phys. (Moscow) **1**, 439 (1939).
[13] Fermi showed [11] that in a dispersive and transparent resonant medium emission can occur at arbitrarily small velocities owing to the fact that the threshold velocity square, proportional to $c^2/\epsilon(\omega)$, may become quite small in concomitance with a resonance.
[14] H. Motz and L. Schiff, Am. J. Phys. **21**, 258 (1953).
[15] I. Frank, JETP Lett. **28**, 446 (1978).
[16] I. Frank, Nucl. Instrum. Methods Phys. Res. A **248**, 7 (1986).
[17] I. Carusotto, M. Artoni, G.C. La Rocca, and F. Bassani, Phys. Rev. Lett. **87**, 064801 (2001).
[18] G. Afanasiev, V. Kartavenko, and E. Magar, Physica B **269**, 95 (1999).
[19] T. Stevens, J. Wahlstrand, J. Khul, and R. Merlin, Science **291**, 627 (2001).
[20] M. Born and E. Wolf, *Principles of Optics*, 6th ed. (Pergamon Press, Oxford, 1993).
[21] This relation, which expresses the familiar condition for the emission of Cherenkov radiation [5], can also be interepreted from a quantum mechanical standpoint as a direct consequence of the energy-momentum conservation.
[22] When a surface between different media or a medium and the vacuum are considered, a charged particle may also excite surface modes and emit transition radiation (See, e.g., L.D. Landau and E.M. Lifschitz, Ref. [5], Sec. 84). These effects, which are important in a thin slab configuration, are, however, not relevant to the infinite geometry situation examined here.
[23] We adopt such a coordinate system as we are here mainly interested in the effects of an external electric field on the resonant emission yield of Cherenkov radiation and only partly in its geometrical properties. These properties are typically described by taking instead the polar axis of the wave vector $\boldsymbol{k}$ to coincide with the cone axis [4].
[24] J. Jackson, *Classical Electrodynamics*, 2nd ed. (Wiley, New York, 1975), Sec. 6.8. Note that it is in this case the charge current itself that generates the bulk electric field **E**.
[25] E. Tosatti and F. Bassani, Nuovo Cimento B **65**, 161 (1970).
[26] Cherenkov losses are clearly absent for very small velocities.
[27] K. Zeppenfeld, Z. Phys. **211**, 391 (1968).
[28] F. Bassani and E. Tosatti, Phys. Lett. **27A**, 446 (1968).
[29] E. Tosatti, Nuovo Cimento B **63**, 54 (1969).
[30] Note again that Eq. (19) refers to the overall loss due to both transverse and longitudinal volume excitations of the field.
[31] F. Bassani and G. Pastori Parravicini, *Electronic States and Optical Transitions in Solids* (Pergamon Press, Oxford, 1975).
[32] P. Yu and M. Cardona, *Fundamentals of Semiconductors* (Springer, Berlin, 1996).
[33] M. Artoni, G.C. La Rocca, and F. Bassani, Europhys. Lett. **49**, 445 (2000).
[34] D. Fröhlich, A. Nothe, and K. Reimann, Phys. Rev. Lett. **55**, 1335 (1985).
[35] D. Fröhlich, Ch. Neumann, B. Uebbing, and R. Wille, Phys. Status Solidi B **159**, 297 (1990).
[36] M. Artoni, G.C. La Rocca, I. Carusotto, and F. Bassani, Phys. Rev. B **65**, 235422 (2002). See also Ref. [33] where we examined only one choice of polarization assuming well isolated Γ_4^- states.
[37] The three numbers in the square brackets are as usual proportional to the components of the polarization unit vector along the material cubic axes.
[38] S. Nikitine, J.B. Grun, and M. Sieskind, J. Phys. Chem. Solids **17**, 292 (1961); *Semiconductors*, Landolt-Börnstein, New Series, Group III, Vol. 17 (Springer, Berlin, 1984).
[39] *Semiconductors*, (Ref. [38]).
[40] This, in particular, generalizes preliminary work on the possibility of enhancing Cherenkov emission at normal incidence [see, M. Artoni, I. Carusotto, G.C. La Rocca, and F. Bassani, Z. Naturforsch., A: Phys. Sci. **56**, 169 (2001)].
[41] Even stronger enhancements can be attained by using an off-resonant external field of the same intensity (see, Ref. [33]).
[42] This can be easily verified by expanding $\epsilon_\parallel$ and $\epsilon_\perp$ in Eq. (27) in the exciton resonance region so as to obtain with the help of Eq. (7) $\mathrm{Im}[\epsilon_r] \approx 10^{-3}$ and likewise small values for $\mathrm{Re}[\epsilon_r]$. The same holds when the tensor (29), corresponding to the other external field configuration, is used.
[43] The situation may be considerably improved in ultracold alkali atoms, e.g., where typically D_1 or D_2 transitions are rather strong with a concomitant bulk index ϵ_∞ that is nearly unity [see, e.g., M. Artoni, G. La Rocca, F. Cataliotti, and F. Bassani, Phys. Rev. A **63**, 023805 (2001)].
[44] Our situation resembles that of the emission of Cherenkov radiation in a magnetized plasma, where the presence of an external magnetic field, instead of an electric one, leads to a plasma anisotropy with two temperatures parallel and perpendicular to the magnetic field direction. In a similar way, yet with different results, the anisotropy arising from the two different temperatures modify the dielectric tensor and subsequently the Cherenkov emission spectrum [see, e.g., F. Moser, T. Nguyen, and E. Rauchle, Kerntechnik **61**, 183 (1996)].
[45] Early work on the emission of Cherenkov radiation in anisotropic nondispersive and transparent media goes back to Ginzburg and Pafomov who studied the phenomenon, respectively, in nonmagnetic and magnetic (ferrite) materials. See, V. Ginzburg, JETP **10**, 608 (1940); V. Pafomov, Sov. Phys. JETP **3**, 597 (1956).
[46] See, e.g., L.D. Landau and E.M. Lifschitz (Ref. [5]), Secs. 76–78.
[47] Here again, as in Sec. III, we consider a range of resonant frequencies for which the real parts of the two tensor components $\epsilon_\parallel$ and $\epsilon_\perp$ are much larger than the corresponding imaginary parts that are than neglected.